

Feasibility to add a hemispherical energy analyzer to PEEM3 as an imaging energy filter

Jun Feng, Alastair MacDowell and Howard A. Padmore
ESG, ALS
Lawrence Berkeley National Lab.
12/2002

1. Introduction

The combination of high spatial resolution microscopy with measurement of photoemission electron energy distribution is called spectromicroscopy. Adding an imaging energy filter to X-PEEM, not only excitation source can be variable to have elemental resolved image, but also chromatic aberration is greatly reduced. In the case of the aberration corrected PEEM, the long tail of the emitted secondary electron energy distribution will make the aberration correction imperfect and diffraction will limit the best resolution (so far 5nm at object side for PEEM3). The energy filter will eliminate the long tail of secondary electron distribution and improve the resolution (0.5nm based on SMART project). During the past years, substantial efforts have been undertaken in order to design imaging energy filters for PEEM, such as 90⁰ or 180⁰ electrostatic prisms [1-2], Omega magnetic filter[3], crossed field electro-magnetic Wien filter[4] and also a multipole version[5].

During the process in the design of PEEM3, one consideration is the feasibility of adding an imaging energy filter to PEEM3. The question posed - “is it worth doing a major study if the solution is just to simply design the PEEM3 chamber bigger and leave some space for an energy filter”. Due to the consideration of nominal simplicity and inexpensive, we choose the electrostatic Hemispherical Energy Analyzer (HEA) as our candidate energy filter.

2. Principle of hemispherical energy analyzer

The Hemispherical Energy Analyzer (HEA) is an electrostatic device used to disperse electrons as a function of their kinetic energy. It is analogous to a prism, which disperses light depending on its wavelength. It is widely used in electron spectroscopy due to favorable inherent focusing properties and ease of construction. The HEA consists of two concentric spheres with an applied voltage V_{in} for the inner shell and V_{out} for outer shell :-

$$V_{in} = 2E_0 \left(\frac{R_0}{R_{in}} - 1 \right), \quad V_{out} = 2E_0 \left(\frac{R_0}{R_{out}} - 1 \right) \quad (1)$$

Where E_0 is the energy of the electrons (pass energy) with radius R_0 , R_{in} and R_{out} are inner and out shell radius, respectively. The voltage difference between the two shells is

$$\Delta V = E_0 \left(\frac{R_{out}}{R_{in}} - \frac{R_{in}}{R_{out}} \right) \quad (2)$$

Eq.(2) shows that the dimension of the HEA is related with the pass energy. Normally, the outer shell radius is about 10-20cm, and the gap is about 40cm due to the consideration of collecting as big as possible angle acceptance for spectroscopic use.

Neglecting the fringe field, to a low order approximation, the radial and azimuthal position (x_i, y_i) and angle (α_i, β_i) of an electron at the exit plane is:

$$\begin{aligned} x_i &= -x_0 + 2\delta - 2\alpha^2_0 & \alpha_i &= -\alpha_0 \\ y_i &= -y_0 & \beta_i &= -\beta_0 \end{aligned} \quad (3)$$

where δ is energy difference ratio defined as $\delta=(E-E_0)/E_0$, E is the electron energy and E_0 is the pass energy.

Eq.(3) shows the first order focusing (in terms of α) along the dispersion axis, and perfect focusing in the non-dispersive axis. The left panel in fig. 1 shows the dispersion plan of a hemispherical capacitor, together with three computed electron trajectories for different energies by SIMION. The right panel shows the focus properties of the HEA for different angles.

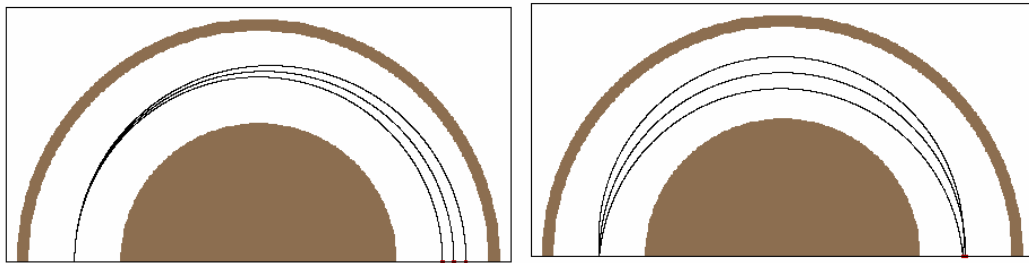


Fig.1. Focus of the HEF. Left panel: electrons with energies $(E_0-\delta, E_0, E_0+\delta)$ are dispersed at exit plan. Right panel: Electrons with different angles $(\alpha_1, \alpha_2, \alpha_3)$ are focused at exit plan to first order.

Fig.2 shows the trajectory and dispersion for 1kev electron in a hemispherical capacitor with 80mm mean path radius. To make a photoelectron spectrometer, one places a detector to collect the electrons which arrive at position x_i with energy δ .

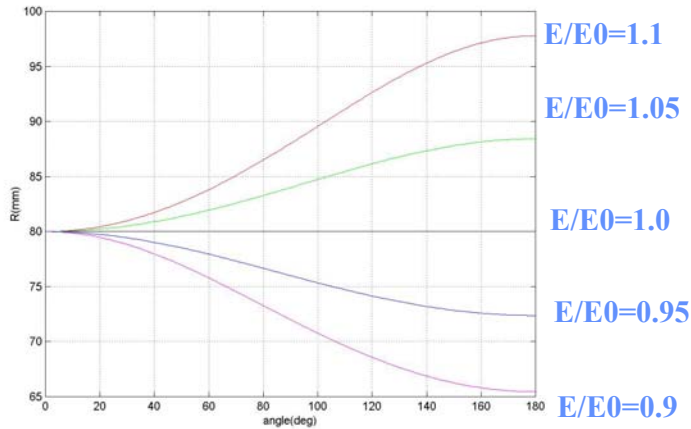


Figure 2 Trajectory and dispersion of 1kev electron at 80mm mean path HEF

3. Principle of the HEA as an imaging energy filter

While the use of the HEF for spectroscopy is clear, it is less obvious how to use it for energy filtered imaging. Tonner [1] points out that the energy-filtering process of the HEA

will not disturb the image if the two dimensional intensity map of object $I(x,y)$ can be mapped into the angle-space $I(\alpha,\beta)$. He also proposed to use two coupling lenses at the entrance plan and exit plane to accomplish this mapping as shown in fig.3. The entrance plane of the hemispherical capacitor is at the back focal plan of coupling lens L1, then the image information at the object side of L1 is mapped as angle distribution at F2. The hemispherical capacitor transfers this angle distribution with magnification one to exit plan F1 with energy dispersion. Finally, coupling lens L2 maps the angle distribution back to image distribution at F2.

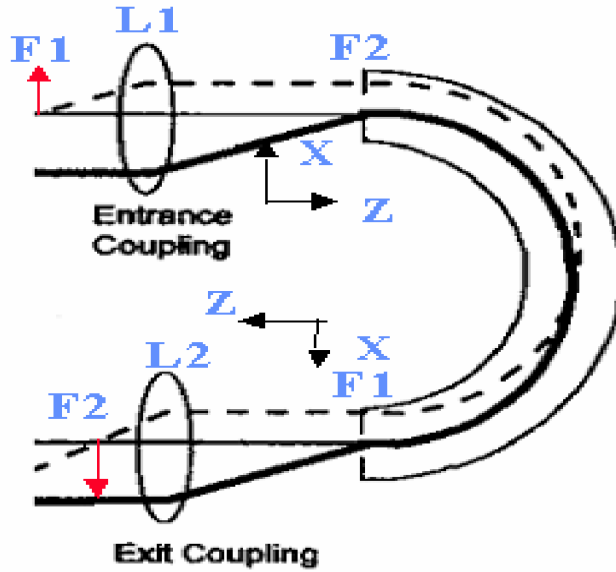


Figure.3 Schematic of HEA as image preserving energy filter[6]. The focal plane of coupling lenses are at the entrance and exit planes of the HEA

If s is the object size of coupling lens L1, then the angle and size of the electron beam at the entrance plane are determined by [6]

$$\begin{aligned} r_{ent} &= \alpha_{pencil} f \\ \alpha_{ent} &= s / f \end{aligned} \quad (4)$$

where f is the focal length shown in figure 4

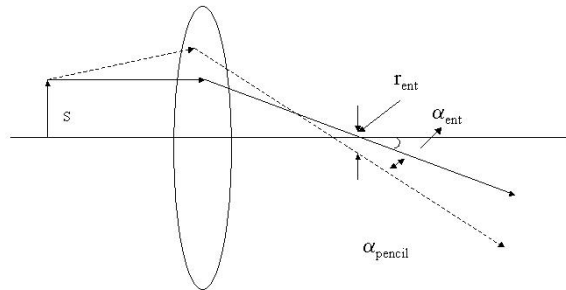


Figure 4. Position to angle mapping by coupling lens

Based on the resolution of CCD camera with 1kx1k size, the following criteria must be satisfied when using the HEA as imaging energy filter for high resolution of PEEM3 requirement:

- 1) for position to angle mapping by coupling lens

$$\frac{d\alpha_{ent}}{\alpha_{ent}} < \frac{1}{1024} \quad (5)$$

- 2) For angle to angle mapping by the HEA

$$\frac{d\alpha_{exit}}{\alpha_{exit}} < \frac{1}{1024} \quad (6)$$

4. Aberration calculation

Based on eq.(5-6) for requirements of spatial resolution, the aberrations for the coupling lens and the HEA must be calculated for PEEM3.

1) The linearity of mapping position to angle of an uni-potential electrostatic lens

The lens is same as the PEEM3 transfer lens except that it is operated at 613.4145 volts and has a focal length $f=31.81\text{mm}$. This is because a deceleration ratio 20:1 is used, similar to Tonner's paper [6]. Electrons are fired parallel with different displacements into the lens within SIMION and record the angles of the rays at the back focal plan of the lens. The linearity of mapping position to angle of the lens is shown in figure 5.

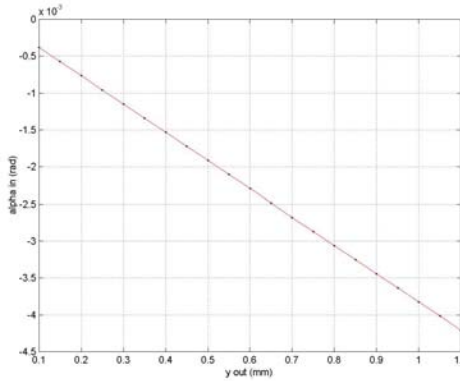


Figure 5 linearity of mapping position to angle by lens

The curve of figure 5 can be fitted with the following equation

$$\alpha_{out} = -0.038Y_{in} - 2.4476 \times 10^{-6} Y_{in}^2 \quad (7)$$

From eq (5), $\frac{2.4476 \times 10^{-6} Y_{in}^2}{0.038 Y_{in}} \leq \frac{1}{1024}$, the object size in front of the lens should be smaller than 1.516mm.

Since $\alpha_{ent} = s / f$, if the coupling lens has longer image side focal length, then the beam angle will be smaller. We also checked the linearity of mapping position to angle for

different focal length. For $f \sim 71\text{mm}$, $V = -500\text{v}$,

$$\alpha_{out} = -0.0018Y_{in} - 1.1876 \times 10^{-6} Y_{in}^2, Y_{in}^2 \frac{1.1876 \times 10^{-6} Y_{in}^2}{0.0018Y_{in}} \leq \frac{1}{1024}, \rightarrow Y_{in} < 1.4799\text{mm};$$

For $f \sim 100\text{mm}$, $V = -438.3\text{v}$,

$$\alpha_{out} = -0.0012Y_{in} - 8.521 \times 10^{-7} Y_{in}^2, \frac{8.521 \times 10^{-7} Y_{in}^2}{0.0012Y_{in}} \leq \frac{1}{1024}, \rightarrow Y_{in} < 1.3753\text{mm}.$$

It can be seen that the allowable object size is becoming smaller when focal length becoming longer due to the linearity of the lens. So the focal length $f = 31.81\text{mm}$ is chosen.

2) The aberration of 180 deg hemispherical capacitor

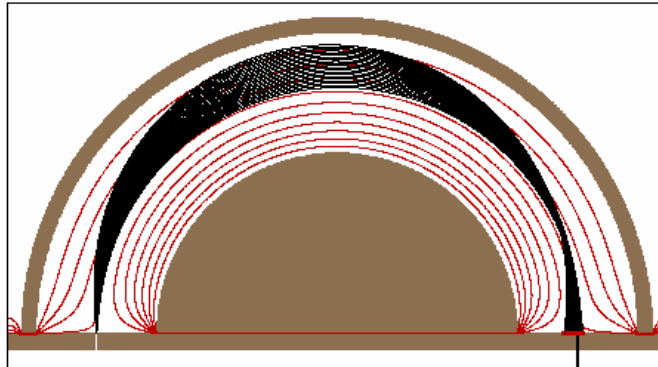


Figure 6 Equipotential distribution of a 180 deg hemispherical capacitor by SIMION. The fringe field is clearly seen at the entrance and exit regions

Figure 6 shows the equipotential distribution of the hemispherical capacitor with fringing fields. The outer shell radius is 10cm, which is referred from E.Bauer [7]. The gap is 40mm, which is typical in commercial HEA. The mean pass energy is 1keV, and the voltages are $V_{in} = 667.2145\text{v}$, $V_{out} = -400\text{v}$. The potential distribution is shown in figure 7 and it has the form of $P = \frac{1.597 \times 10^{-5}}{r} - 1.5955 \times 10^{-3}$, which is same as analytical predication.

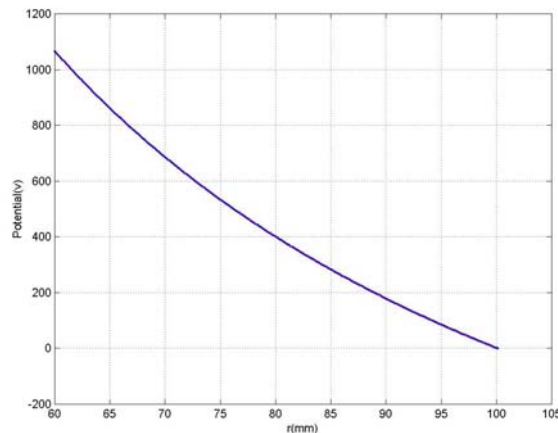


Fig.7. Potential distribution of the hemispherical capacitor

Figure 8 shows the relationship between the entrance angle and exit angle by the hemispherical capacitor. It gives how good the hemispherical capacitor can map the angle distribution to the exit plane of the hemispherical capacitor.

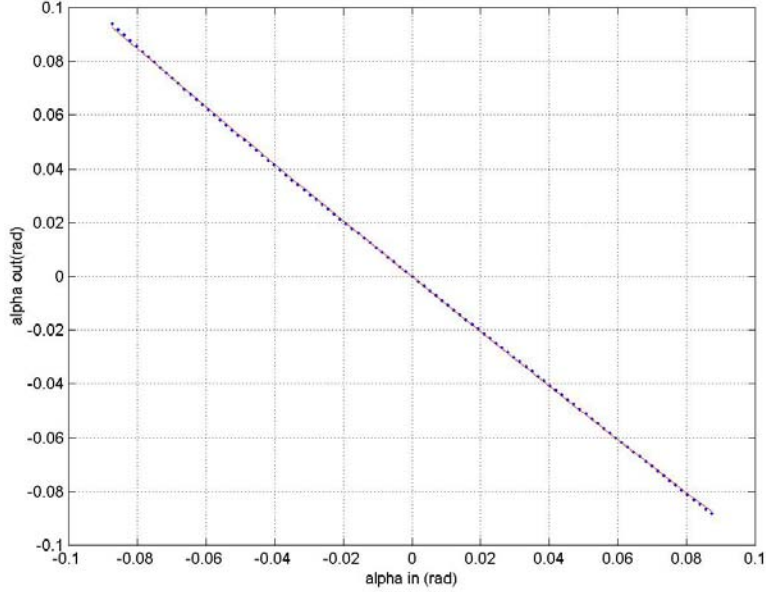


Fig 8 Angle to angle mapping by hemispherical capacitor

Fitting the results of figure 8, we obtain the following equation

$$\alpha_{out} = -1.0329\alpha_{in} - 0.3511\alpha_{in}^2 \quad (8)$$

The first term in eq.8 gives the angle magnification, which is ~ -1 , the same as predicated by eq.3. The second term is the aberration which causes the exit angle to vary the entrance angle. The fringe field is the main contributor to the aberration and is difficult to calculate by analytical methods, but relative easily done by SIMION.

From eq (6), $\frac{0.3511\alpha_{in}^2}{1.03292\alpha_{in}} \leq \frac{1}{1024}$, - states the entrance angle should be smaller than

$2.873 \times 10^{-3} \text{ rad}$. Putting this number in eq.(4), $\alpha_{beam} = \frac{s}{f} \leq 2.873 \times 10^{-3}$ and $f = 31.81 \text{ mm}$, we obtain the object size in front of the lens, which should be smaller than $91.936 \times 10^{-3} \text{ mm}$. This is much smaller than the requirement by the coupling lens.

The steps of decelerating the electrons from the high voltage section energy 20keV to the pass energy 1keV results an increase in the electron pencil angles of a factor of $\sqrt{\frac{20000}{1000}} = 4.5$. The effect of this increase is small which can be seen from the following calculation. The pencil angle at the virtual image plane of the extracting field is typically around 6.4 mrad. Assuming an overall magnification $m=10$ (which is a typical number for the PEEM objective lens), then the pencil angle after the deceleration section is

$$\alpha_1 = \frac{2/3}{M} \alpha_0 \sqrt{\frac{E_{acc}}{E_p}} = 1.91 \text{ mrad} \quad (9)$$

This gives the beam size at the entrance plan of hemispherical capacitor $r_{ent} = 1.91 \text{ mrad} \times 31.81 \text{ mm} = 60.728 \mu\text{m}$, which is very small.

5. Results and discussion

For PEEM3 it is proposed that there be two operation modes. For high resolution mode, the field of view is $5 \mu\text{m}$, compared with $91.936 \mu\text{m}$, magnification $m = 91.936/2.5 = 36.77$ is acceptable. But for high flux mode, the field of view is $40 \mu\text{m}$, then only magnification $m = 4.6$ is acceptable. This makes it difficult to add HEA to PEEM3 since PEEM3 objective lens has 12 magnification.

It is well known that the aberration can be reduced by eliminating the fringe field of the HEF using Jost correction [8], reducing the gap or paracentric entry [9]. It is profitable to check the angle mapping aberration of an ideal hemispherical capacitor with fringe field correction in order to see if it can satisfy the resolution requirement of PEEM3. Figure 9 is equipotential distribution of an ideal hemispherical capacitor without fringe field errors. It clearly shows that the focus plane moves to the exit plan of hemispherical capacitor. Compare to Fig.6 which shows the focus plane before the exit plane with fringing fields. Figure 10 shows the relationship between the entrance angle and exit angle for this ideal hemispherical capacitor.

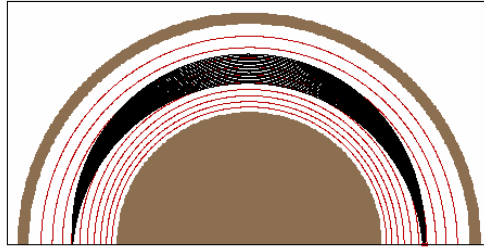


Fig.9 Hemispherical capacitor without fringe field

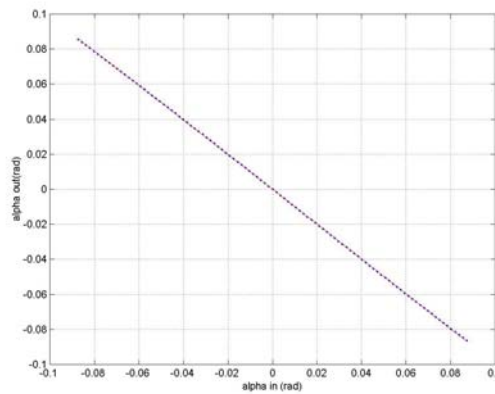


Fig.10 Angle mapping aberration for an ideal hemispherical capacitor

From fig.10 can be represented by the following equation

$$\alpha_{out} = -0.9906\alpha_{in} - 0.066\alpha_{in}^2 \quad (10)$$

Comparing with eq.(8), it can be seen that the angle magnification is still one, but the aberration reduces more than a factor of 5.3. This leads to an increase in entrance angle to $\alpha_{in} = 0.01466rad$ (from $\frac{0.066\alpha_{in}^2}{0.9906\alpha_{in}} \leq \frac{1}{1024}$). Projecting back to the object size in

front of the coupling lens, it is 0.466 mm (from $\frac{s}{f} \leq 0.01466$ and $f = 31.81\text{ mm}$). For

high resolution mode of PEEM3, field of view is $5\text{ }\mu\text{m}$, compared with $S < 466\text{ }\mu\text{m}$, front end magnification $m=186.4$ is accepted. For high flux mode, field of view is $40\text{ }\mu\text{m}$, compared with $S < 466\text{ }\mu\text{m}$, magnification $m=23.3$ is accepted. Although this HEA can not be simple add-on to the end of PEEM3 either even for ideal filter due to tens thousand magnification of PEEM3, it can be put behind the first transfer lens after the separator. Actually, that the conclusion of HEA can not be simply hooked up to the end of PEEM3 is obvious since the image size over there is in several cm order and the HEA is only 10 cm. By reducing the HEA gap to 20mm from 40mm, the aberration will be also much reduced, then magnification $m=75.8$ is acceptable, and this gives more space choosing flexibility to add HEA to PEEM3.

The deceleration telescope and acceleration telescope are another critical elements from the point of view of spatial resolution and distortion[6]. The telescope can be equally treated as a single, four-element complex lens. The equi-potential distribution of this telescope lens is shown as fig.11. The first three electrodes is conventional uni-potential lens with the image side point coincident with the object side focal point of the retarding lens.

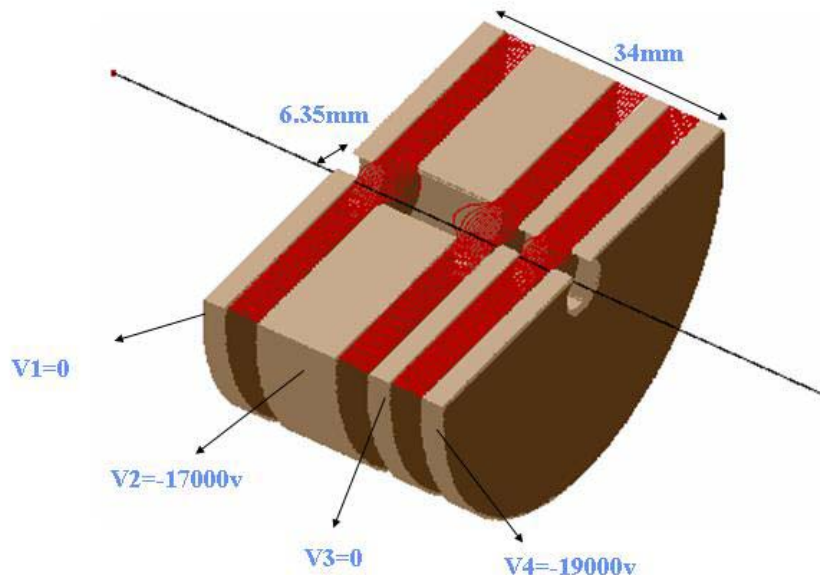


Fig.11 Retarding electron telescope complex lens

If we name the two retarding lens telescope, two coupling lens and hemispherical capacitor as imaging filter section, Fig.12 shows the electron trajectory for the imaging filter section. To reduce the size of the hemispherical capacitor, the electrons are decelerated with a ratio 20:1 by the deceleration telescope section. After the hemispherical capacitor, the electron is accelerated back to high voltage with same ratio 1:20 by an acceleration telescope section. In fig.12, the entrance center path of hemispherical filter is located at $y=80\text{mm}$, which is the entrance optics axis. And the exit center path is at $y=-80\text{mm}$, which is the exit optics axis after 180 degree bending. A 20keV electron with 1mm size parallelly entered the imaging filter section at displacement $y=79\text{mm}$, it is decelerated to 1keV with unit magnification and is located at $y=81\text{mm}$ and parallelly entered the coupling lens. The coupling lens focused it at $y=80\text{mm}$ the entrance center path of hemispherical capacitor. The coupling lens at the exit side of hemispherical filter and acceleration retarding lens reverse the above process. It can be seen from the figure the finally exit electron had 20keV energy back and landed at $y=-79\text{mm}$, which gives unit magnification.

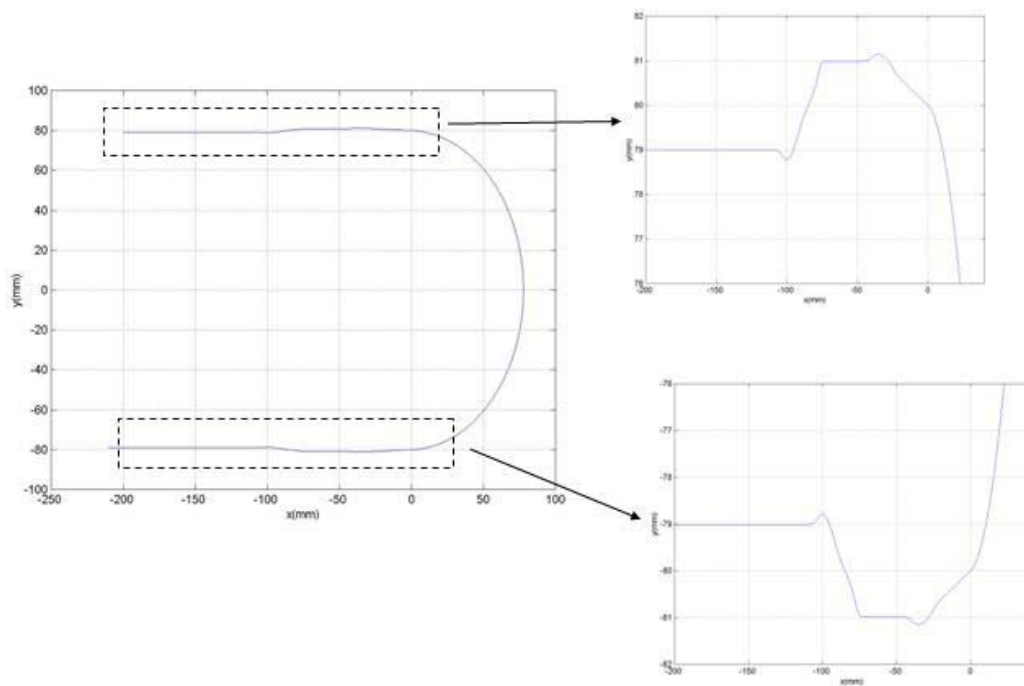


Fig.12 Electron trajectory calculation of imaging filter section

The high voltages for all the electrodes of imaging filter section are shown in figure 13. Due to the retarding lens, the outer electrodes of coupling lens are not grounded. Also the energy filter is on high voltage. This makes the high voltages connection very complicated.

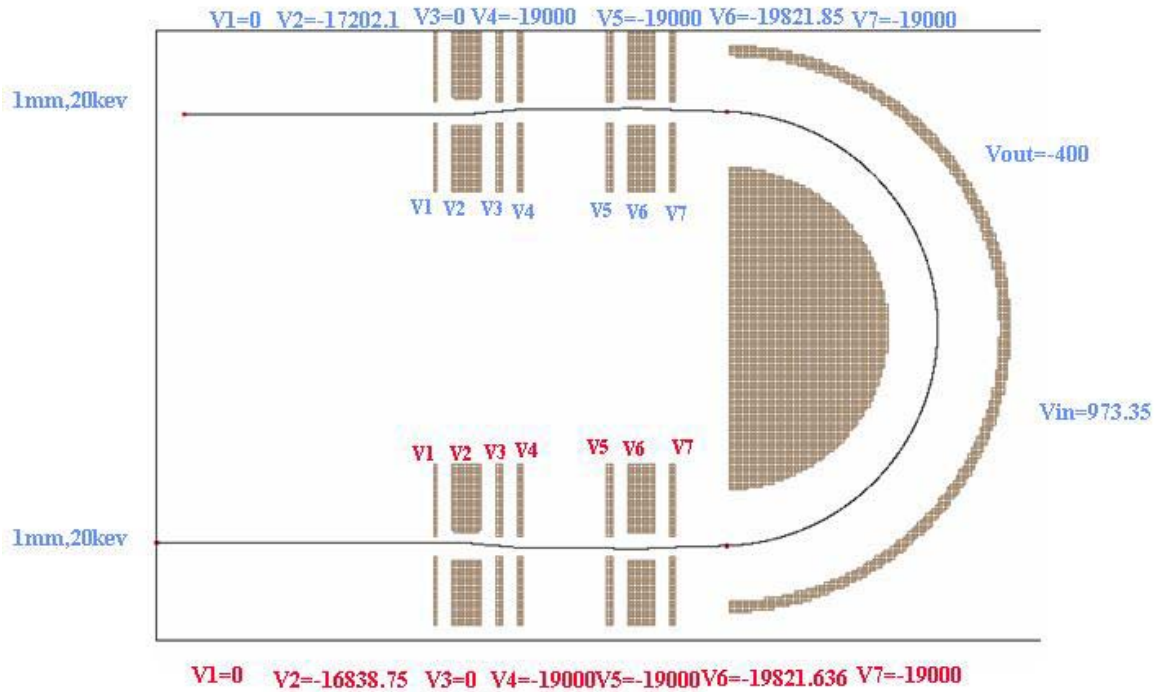


Fig.13 high voltage connection for the imaging energy filter section

Based on the current PEEM3 design, fig.14 is a possible layout of PEEM3 with an imaging energy filter.

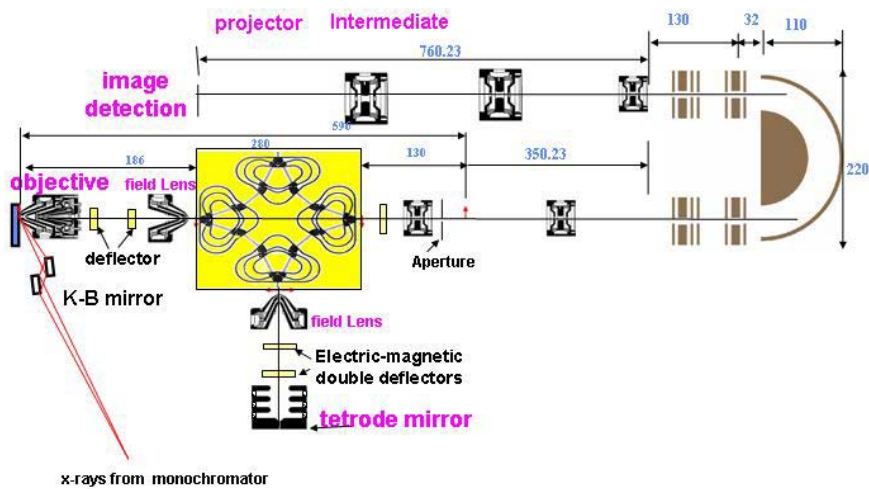


Fig.14 The possible layout of PEEM3 with a hemispherical imaging energy filter

The current PEEM3 design is split between the transfer lens and the first intermediate lens and the hemispherical image filter section is inserted. Due to the length of magnifying and projector column, another transfer lens with unit magnification is used to transfer the image with 360.23mm distance to put the CCD detection plan on the entrance plan of separator, which makes PEEM3 separator chamber design easy.

In summary, we have checked the focus and dispersion properties of a hemispherical capacitor both using ray tracing and analytical methods. The linearity of mapping position to angle by an unipotential electrostatic lens and the aberrations of mapping the angle by a hemispherical capacitor have been calculated. These factors determine the feasibility of adding a hemispherical energy filter to PEEM3 as an image energy filter. By designing a hemispherical capacitor with small fringe field and small gap, a hemispherical capacitor with two coupling lens and two electron retarding telescopes can be used as an image filter for PEEM3. It is also seen that this new PEEM3 instrument becomes much more complicated. Also more work needs to be done in the future such as finding the best way to reduce the fringe field effect of hemispherical capacitor. Furthermore it is also very interesting to compare the possibility and complexity of using an Omega type magnetic filter to PEEM3 since in this case it is not necessary to decelerate the electrons or use coupling lenses, and many aberrations will be cancelled out due to the symmetry of the Omega type filter.

Reference:

- [1] B.P.Tonner, Nucl.Instr.Meth. A291(1990)51
- [2]L.H.Veneklasen, Rev.Sci.Instrum. 63(1992)5513
- [3]S.Lanio, H.Rose, D.Krahl, Optik, 73(1986)56
- [4]K.Tsuno, Rev.Sci. Instrum, 64(1993)659
- [5]G.K.L.Marx, V.Gerheim, G.Schönhense, J. Electron Spectrosc. Relat. Phenom. 84(1997)251
- [6] B.P.Tonner, D.Dunham, T.Droubay, M.Pauli, J. Electron Spectrosc. Relat. Phenom. 84(1997)211
- [7]E.Bauer, private communication
- [8]K.Jost, Rev.Sci.Instru., 12(1979)1001
- [9]T.J.M.Zouros, E.P.Benis, J. Electron Spectrosc. Relat. Phenom. 125(2002)221